

Fig. S7

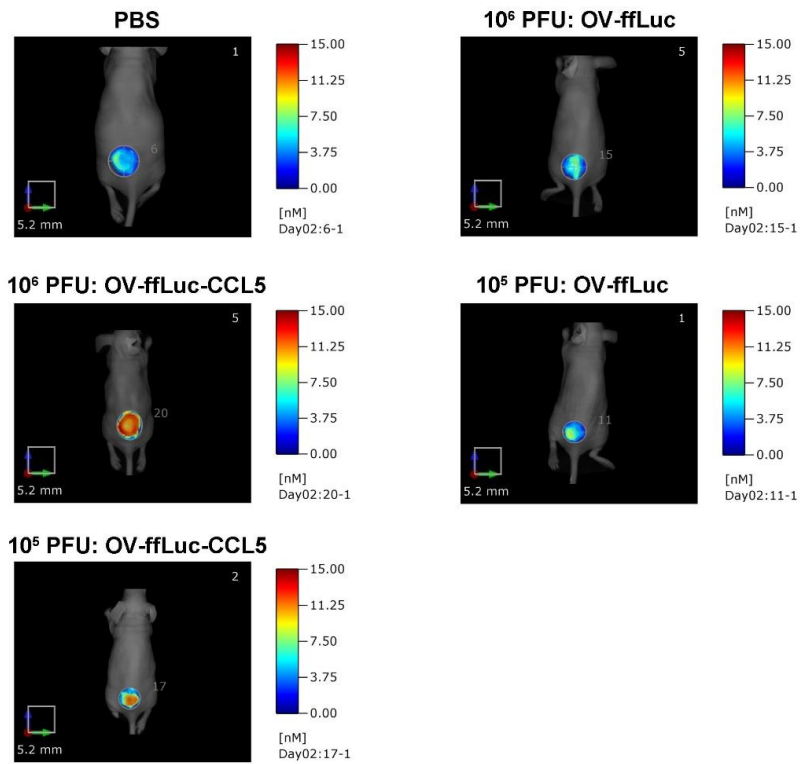


Figure S1. Characterization of NK cells. **a**, Purified (day 0) and expanded (day 15) NK cells were phenotyped by FACS analysis. **b**, Gating strategy for analyzing GFP and CCR5 expression in NK cells from Fig. 1B. **c**, Proliferating curves of NK cells that were gene modified or not. NK cells expansion folds were determined on day 4, 7, and 15. Data shown are representative of assays with samples from at least five healthy subjects.

Figure S2. Apoptotic death of tumor cells induced by NK cells. Tumor cells were mixed with NK cells at E:T = 1:1 for 6 h. Apoptotic tumor cell ratios were determined by Annexin V/PI staining.

Figure S3. Effect of OV infection on NK cells. **a**, NK-CCR5 cells were infected with OV-ffLuc or OV-ffLuc-CCL5 at MOI = 1. Twenty-four and Forty-eight hours later, cells were washed with PBS for 3 times and DNA samples were prepared. Next, 100 ng DNA was used to detect OV genome within NK cells by real-time PCR. Negative control, NK-CCR5 cells pre-treated with PBS alone; positive control, 5 ng DNA isolated from HCT-116 cells infected with OV-ffLuc at MOI = 0.1 for 24 h. **b**, Tumor cells were incubated with NK-CCR5 cells pre-treated with the indicated virus, after which tumor cell apoptosis was determined 6 h later. **c**, Pretreated NK-CCR5 cells were co-incubated with tumor cells at E:T = 1:1 for 24 h, after which ELISA was performed to analyze effector cytokines in supernatants. NK cells were collected from five donors. * $P < 0.05$, *** $P < 0.005$ (one-way ANOVA).

Figure S4. NK cell infusion had limited effect on vaccinia virus replication *in vivo*. As depicted in Fig. 6A, nude mice subcutaneously inoculated with HCT-116 cells

were sequentially injected with oncolytic virus and NK-CCR5 cells ($n = 3$). Virus replications *in vivo* were monitored using the IVIS imaging system on days 1, 3, 5 and 10. BLI demonstrated that the persistence of oncolytic vaccinia virus was limited and that NK cells barely had an impact on virus expansion. One-way ANOVA analysis was performed to compare the differential BLI intensities.

Figure S5. Accumulation of NK cells within tumor tissues. Following the procedure described in Fig. 6A, nude mice were sequentially treated with OV and NK-CCR5 cells. Mice were sacrificed and tissues collected on day 6, 9, 14, and 24 ($n = 4$ at each interval per treatment). Tissues were dispersed and the single cell suspensions were stained with fixable viability dye and anti-human CD45 antibody conjugated with fluorochrome. Next, the samples were subjected to FACS analysis. **a**, Gating strategy. Cells were collected according to FSC/SSC, following which live cells were gated according to viability dye staining. Afterwards, NK cell ($CD45^+$) accumulation within live cells was determined. **b**, NK cell accumulation in the liver, lung, spleen, and tumor tissues at the indicated time points. $*P < 0.05$, $***P < 0.005$ (one-way ANOVA).

Figure S6. Accumulation of NK cells within tumor tissues. HeLa cells were inoculated subcutaneously into nude mice. When tumor volumes reached $\sim 100 \text{ mm}^3$, 10^5 or 10^6 PFU of the indicated virus were intratumorally injected ($n = 4$ per group). Four days later, 5×10^6 NK-CCR5 cells were infused intravenously. At the indicated time points, tumor tissues were isolated and dispersed. The prepared single cell suspensions were incubated with fixable viability dye and fluorochrome-conjugated

anti-human CD45 antibody. Samples then were subjected to FACS analysis. $*P < 0.05$,

$**P < 0.0$, $***P < 0.005$ (one-way ANOVA).

Figure S7. Uncropped graphs related to Figure 6E.